Quantum Electronics **51** (5) 427–432 (2021)

CONTROL OF LASER RADIATION PARAMETERS https://doi.org/10.1070/QEL17549

High-frequency pulse train generation in dispersion-decreasing fibre: using experimental data for the metrology of longitudinally nonuniform fibre

I.S. Panyaev, D.A. Stoliarov, A.A. Sysolyatin, I.O. Zolotovskii, D.A. Korobko

Abstract. **This paper describes experiments concerned with pulse train generation from initially modulated cw light in an anomalous dispersion decreasing fibre. We have obtained stable contrast trains of subpicosecond pulses with a repetition rate in the range 100–300 GHz and demonstrated generation of an optical comb spectrum with a –20-dB width of up to 80 nm. A method has been proposed for reconstructing an unknown dispersion profile of a longitudinally nonuniform fibre by comparing experimental data and numerical simulation results.**

Keywords: *optical fibre, anomalous dispersion, high-frequency pulse train, repetition rate of up to 300 GHz.*

1. Introduction

Modulation instability (MI) is known to be a fundamental nonlinear process that leads to instability growth in physical systems [1]. In optics, this effect can show up as the breaking of a modulated continuous wave into a pulse train. The best known manifestations of MI are those in systems that can be described by equations of the same type as the nonlinear Schrödinger equation (NLSE), e.g. during propagation of a modulated wave in optical fibre [2–4]. Similar processes are observed in optical cavities [5–7], in spatiotemporal laser beam dynamics [8], upon the formation of stable structures in waveguides, etc. [9–11].

MI is often a parasitic effect leading to growth of noise disturbances and limiting the performance of coherent signal transmission lines [12]. Nevertheless, the use of MI effects is extremely promising for generating trains of high-frequency short pulses [13–15]. In an experimental technique based on so-called induced MI, the input signal results from the summation of light from a pair of cw sources (most frequently, from semiconductor laser diodes) differing in emission wavelength. As a result, the beat frequency of the sum emission signal becomes the repetition rate of the pulses generated by means of MI. Using this method, one can generate pulse trains with repetition rates of hundreds of gigahertz [16], which is well above the maximum pulse repetition rate (PRR) of harmonically mode-locked fibre lasers (under 25 GHz) [17, 18] and comparable to the repetition rate of pulses generated by significantly more technologically advanced pulsed sources based on semiconductor disc lasers [19] or nonlinear microcavities [20, 21].

The use of dispersion decreasing fibre (DDF), an optical fibre with an anomalous dispersion decreasing along its length, is probably the most effective approach to the generation of high-frequency pulse trains by means of MI [22]. Unlike in the case of longitudinally uniform fibre, the instability frequency range of DDF during light propagation increases steadily, enabling the generation of trains of ultrashort pulses, with a duration considerably shorter than 1 ps, from modulated light [23]. Note that DDFs are highly demanded fibre-optic components: in addition to experimental studies of MI, they are widely used in addressing issues pertaining to laser pulse compression, supercontinuum generation, and optical processing [24–29]. However, there is still no commercial-scale production of such fibres. In experimental studies, use is made primarily of test and research DDF samples fabricated as single pieces, e.g. at the Prokhorov General Physics Institute (PGPI), Russian Academy of Sciences (Moscow) [30]. In connection with this, there is currently great practical interest in the development of DDF metrology methods for high-speed determination of sample characteristics, the most important of which are dispersion parameters.

This paper reports on a series of experiments concerned with the generation of pulse trains by means of MI in a DDF sample prepared in 2020 at PGPI. In these experiments, we were able to obtain subpicosecond pulse trains with a repetition rate above 300 GHz, which to the best of our knowledge is a record for configurations based on a standard silica DDF. (Known results on pulse train generation with a terahertz repetition rate [31] were obtained using a configuration based on a longitudinally uniform, highly nonlinear fibre.) Besides, our experimental data were used to determine the dispersion profile of an experimental DDF sample.

2. Experimental

Figure 1 shows a schematic of the experimental setup. Its key components are two cw laser diodes: a Teraxion stabilised semiconductor laser with an emission linewidth under 10 kHz (DFB1) and a standard Mitsubishi distributed feedback semiconductor laser (DFB2). Varying the drive current and temperature of the laser diodes allows their centre wavelengths to be tuned over a 3-nm range with accuracy no worse than 0.02 nm. After passing through polarisation controllers (PC1, 2) and preamplifiers (EDFA1, 2), the two cw laser beams are

I.S. Panyaev, D.A. Stoliarov, I.O. Zolotovskii, D.A. Korobko
Ulyanovsk State University, ul. L. Tolstogo 42, 432970 Ulyanovsk, Russia; e-mail: rafzol.14@mail.ru;
A.A. Sysolyatin Prokhorov General Physics Institute, Russian Academy of Sciences, ul. Vavilova 38, 119991 Moscow, Russia; Ulyanovsk State University, ul. L. Tolstogo 42, 432970 Ulyanovsk, Russia

Received 2 March 2021
Kvantovaya Elektronika **51** (5) 427–432 (2021)
Translated by O.M. Tsarev

mixed in a 3-dB fibre coupler and 'sliced' by an acousto-optic modulator (AOM) to form 100-ns to 100-μs pulses for effective amplification and suppression of counterpropagating Brillouin-scattered light in the test fibre. Next, the signal is amplified in the main amplifier, EDFA3 (maximum output power of up to 400 mW), and launched into the test fibre (TF). The transmitted light is analysed using an HP 70950B spectrum analyser with a resolution of 0.1 nm and an FR103-WS autocorrelator.

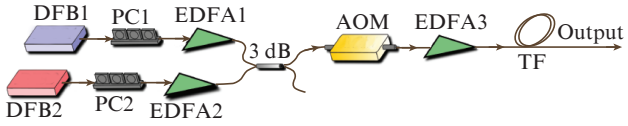

Figure 1. Schematic of the experimental setup: (DFB1, 2) distributed feedback cw semiconductor lasers; (PC1, 2) polarisation controllers; (EDFA1–3) erbium-doped fibre amplifiers; (3 db) 3-dB fibre coupler; (AOM) acousto-optic modulator; (TF) test fibre.

The test fibre used to observe MI effects was a 1000-m length of single-mode silica fibre having a cladding diameter varying linearly along its length. The diameters at the fibre ends were 143 and 114 μm, with the larger diameter corresponding to the maximum anomalous dispersion. The fibre sample was fabricated at PGPI from a preform with a W index profile and had a flat dispersion profile around a wavelength of 1550 nm (i.e. it had a low third-order dispersion). The chromatic dispersion of optical fibre depends on the material and waveguide dispersion contributions. Material dispersion is completely determined by the glass the fibre is made from, and waveguide dispersion depends on the radial refractive index profile (RIP). In the case of the W-profile fibre under consideration, the variation of dispersion along the fibre length is determined by the longitudinal variation of the outer fibre diameter. Thus, if light was launched through the larger end face, the anomalous dispersion of the fibre decreased linearly in the propagation direction [29]. The loss in the DDF was ~1 dB km^{-1}.

In our experiments, amplified modulated light was launched into the DDF through its larger diameter end, which had the highest anomalous dispersion. The average beam power at the DDF input was about 170 mW. Figures 2 and 3 show emission spectra and autocorrelation traces (ACTs) of pulse trains obtained at the DDF output at different modulation frequencies ν. It follows from Fig. 2 that the bandwidth of the comb spectrum depends significantly on ν (i.e. on the wavelength difference $\Delta\lambda$ between the lasers), which can be accounted for by the fact that the modulation gain depends on frequency ν. The comb spectrum has the largest width (–20-dB width of 80 nm) at $\nu \sim 240$ GHz ($\Delta\lambda = 2$ nm). In the central part of the spectrum, the contrast between the lines in the frequency comb and the noise pedestal exceeds 20 dB, pointing to a rather large signal-to-noise ratio of the pulsed source employing MI. The autocorrelation traces in Fig. 3 demonstrate pulse trains with a repetition rate corresponding to the modulation frequency. Note that the central and intercorrelation peaks of the ACTs differ little in intensity, which is characteristic of low-jitter pulse trains [32]. The duration of an individual pulse is ~1 ps, which corresponds to the width of the generated spectrum.

In addition, we carried out experiments in which pulse trains were generated in a two-section fibre consisting of a Corning LEAF standard dispersion-shifted single-mode fibre (3.5 km length) butted against the DDF sample described above. The main idea of the experiment was to use the standard fibre as a medium for pulse train generation by means of MI and the DDF as a compressor in order to reduce the pulse duration and extend the spectrum being generated [26, 27]. The results of that experiment are presented in Fig. 4.

These data demonstrate that the use of a two-section fibre system allows high-frequency pulse trains to be obtained at a lower average power of modulated light. The results presented in Fig. 4 were obtained at an average power at the EDFA3 amplifier output (Fig. 1) near 80 mW. Increasing the power of the modulated light causes no considerable broadening of the comb spectrum being generated. This can be accounted for by the increasing effect of noise factors, which impair the coherence of the output spectrum and emerge in the LEAF fibre, mainly upon dispersion light generation. At the same time, it can be seen that, even at a relatively low average input power, the two-section configuration enables the generation of pulse trains with a repetition rate above 200 GHz and a pulse duration under 1 ps (it should be taken into account that the ACT duration is about a factor of 1.5 longer than the actual pulse duration). It is worth noting that, at a modulation frequency $\nu \sim 120$ GHz (Fig. 4a), there are contrast pulses even after propagation through the LEAF fibre. Propagation through the DDF is accompanied by pulse compression, and the emission spectrum of the pulses broadens. Note also that, despite the low dispersion of the LEAF fibre, its modulation gain range (inversely proportional to its dispersion) is insufficient for contrast pulse formation at a modulation frequency $\nu \sim 240$ GHz (Fig. 4b). In this case, pulse train formation is in effect only due to the development of MI as light propagates through the DDF.

3. Evaluation of dispersion parameters of the DDF

As mentioned above, the ability to determine dispersion parameters of DDFs is a topical issue. It is shown below that dispersion parameters of the DDF sample under study can be estimated by comparing experimental data with numerical simulation results for the MI process. This approach has the following advantages: 1. It offers the possibility of rather rapidly and accurately simulating the propagation of light in optical fibre even on generally available computers using the split-step Fourier method [3], a well-known and long-proven algorithm for solving the NLSE. 2. For metrological measurements on fibre samples, one can use standard experimental setups, e.g. those for optical pulse amplification and compression, without setting up additional systems, often containing expensive bulk components [30]. 3. The proposed approach is nondestructive: it allows one to estimate parameters of an entire sample, which is of particular importance for DDFs. Besides, standard methods for assessing dispersion parameters of optical fibre use small samples, whose dispersion is taken to be constant.

One drawback to the method proposed by us is that it is not self-sufficient, i.e. it needs certain information about parameters of the fibre of interest (effective mode area and longitudinal dispersion distribution), which is used in numerical simulation. At the same time, such information can easily

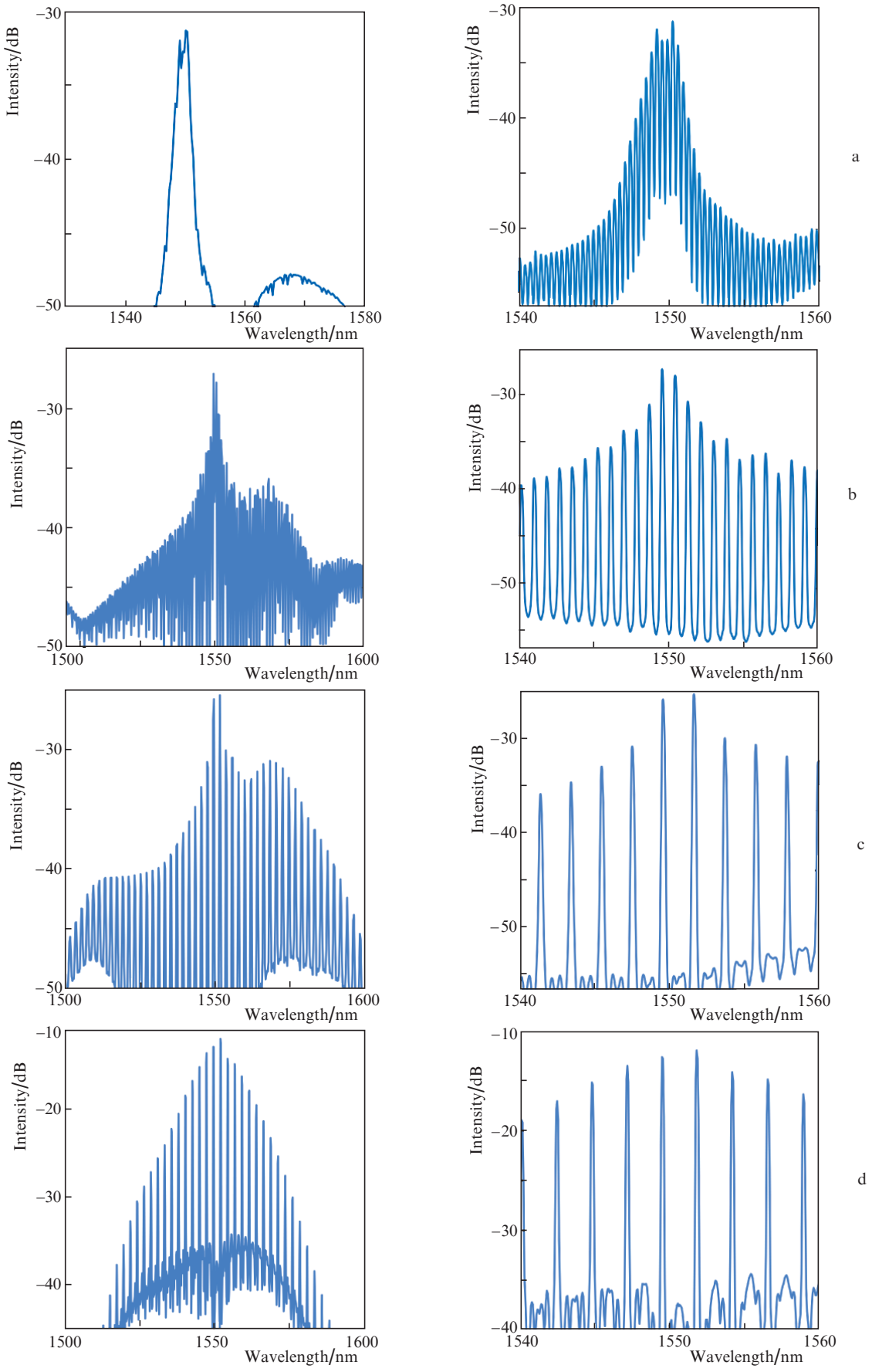

Figure 2. Spectra of the light transmitted by the DDF at modulation frequencies $\nu \sim$ (a) 60 GHz ($\Delta\lambda = 0.5$ nm), (b) 120 GHz ($\Delta\lambda = 1$ nm), (c) 240 GHz ($\Delta\lambda = 2$ nm), and (d) 300 GHz ($\Delta\lambda = 2.5$ nm). The left panels show wide-scan spectra and the right panels show their central parts at a higher resolution.

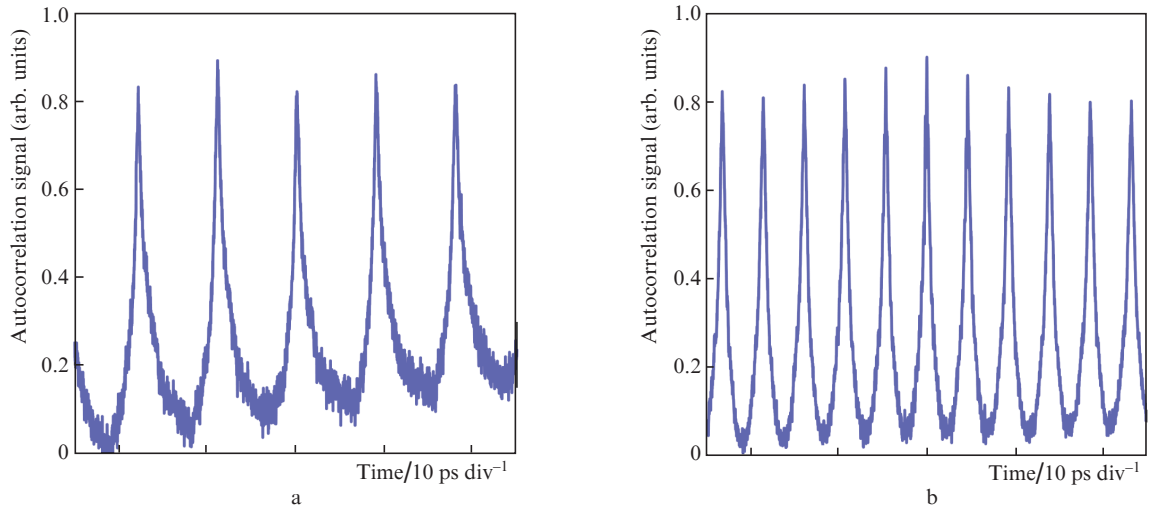

Figure 3. Autocorrelation traces of pulse trains at modulation frequencies $\nu \sim$ (a) 120 GHz ($\Delta\lambda$ = 1 nm) and (b) 240 GHz ($\Delta\lambda$ = 2 nm).

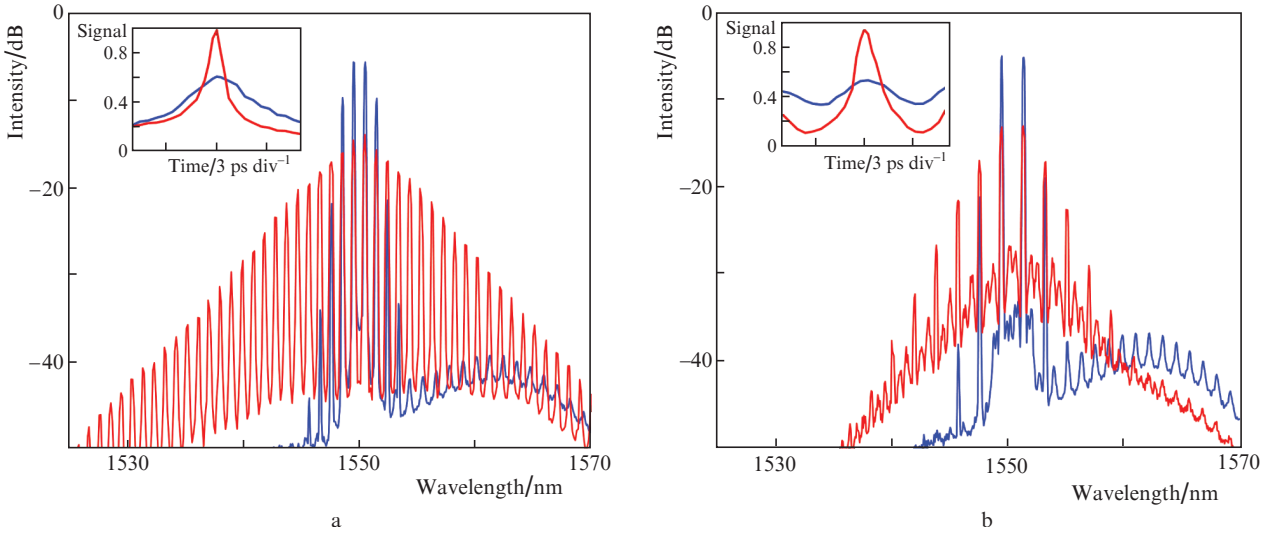

Figure 4. (Colour online) Spectra of light propagating through the Corning LEAF + DDF two-section fibre. Modulation frequency $\nu \sim$ (a) 120 GHz ($\Delta\lambda$ = 1 nm) and (b) 240 GHz ($\Delta\lambda$ = 2 nm). Insets: ACTs of the pulses being formed. The blue lines represent the light that passed only through the LEAF fibre and the red lines represent the light that passed through both sections (Corning LEAF + DDF).

be derived from data on the structure of the sample under study: longitudinal variation in its diameter, core diameter, and core–cladding index difference. Nevertheless, determination of nonlinear characteristics of fibre with a complex W index profile is a nontrivial issue. The main difficulty here is a search for an effective mode area A_{eff} which, together with the nonlinear refractive index n_2 , determines the Kerr nonlinearity coefficient γ of the fibre. In our case, we simplified the problem by representing the complex W index profile as a step-index one, with a core diameter a = 7.5 μm and a core–cladding index difference $\Delta n = 8.5 \times 10^{-3}$. The effective mode area evaluated by the Marcuse formula is $A_{\text{eff}} \approx 52$ μm^2, which eventually allows us to find the Kerr nonlinearity coefficient: $\gamma = 0.0025$ W^{-1} m^{-1}. The fibre cladding diameter has little effect on the effective mode area, so in the approximation in question we take γ to be constant along the length of the fibre.

To find the dispersion profile $\beta_2(z)$ of the DDF, we simulated a solution to the NLSE [3]:

$$\frac{\partial A}{\partial z} + \mathrm{i}\frac{\beta_2(z)}{2}\frac{\partial^2 A}{\partial t^2} - \frac{\beta_3}{6}\frac{\partial^3 A}{\partial t^3} - \mathrm{i}\gamma|A|^2 A = 0, \qquad (1)$$

where $A(z,t)$ is the amplitude of the propagating wave. Initial conditions were inferred from experimental data on the propagation of modulated light in a two-section fibre and corresponded to the radiation pattern at the DDF input (Fig. 4) with allowance for the fusion splice loss (~25% in terms of power). In the initial stage of computation, the third-order dispersion parameter was taken to be $\beta_3 = 0$. Test computations taking into account Raman scattering and self-steepening nonlinear effects [24] showed that they had a negligible effect: the results differed by no more than 0.5%. Because of this, eventually Eqn (1) was simulated with no allowance for these nonlinear effects in order to speed up computations.

The algorithm used to adjust the dispersion profile was as follows: In accordance with the linear variation of the cladding diameter, an unknown dispersion profile, $\beta_2(z)$, was fit-

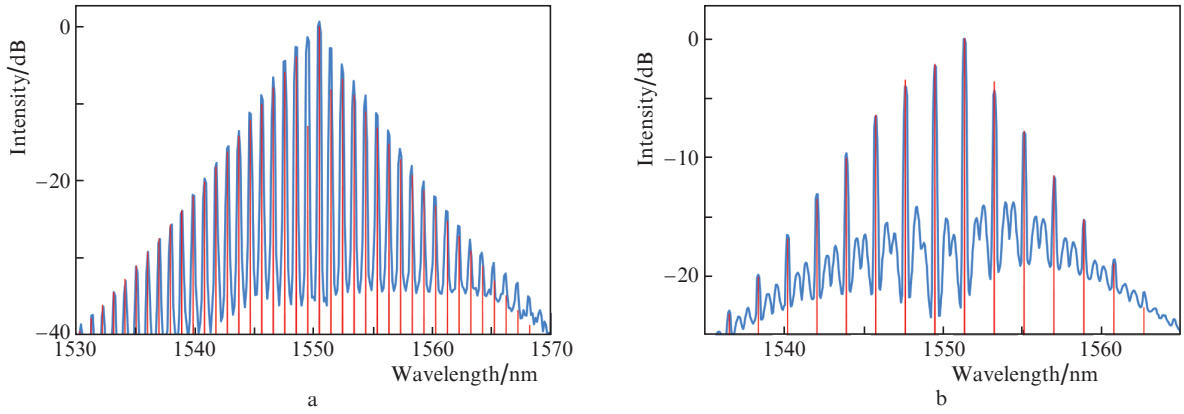

Figure 5. (Colour online) Spectra of modulated light after propagation through the Corning LEAF + DDF two-section fibre. Modulation frequency $\nu \sim$ (a) 120 GHz ($\Delta\lambda$ = 1 nm) and (b) 240 GHz ($\Delta\lambda$ = 2 nm). The blue lines represent experimentally obtained spectra and the red lines represent spectra obtained by simulation with the optimised dispersion profile.

ted by the linear relation $\beta_2(z) = \beta_2(0)(1 - \xi z)$ (where $\xi \approx 10^{-3}$ is an unknown constant), determined by the group velocity dispersion at the input and output ends of the DDF, $\beta_2(0)$ and $\beta_2(L)$. These dispersion parameters were varied in 0.25 ps^2 km^{-1} steps in the ranges $-15 < \beta_2(0) < -2$ ps^2 km^{-1} and $-10 < \beta_2(0) < 5$ ps^2 km^{-1}. The purpose of the computation was to minimise the functional

$$\sum_k \left| I_{\text{th}}(\omega_k) - I(\omega_k) \right|,$$

where

$$I_{\text{th}}(\omega_k) = \frac{\left| A(\omega_k, L) \right|^2}{\max \left| A(\omega_k, L) \right|^2}$$

is the calculated relative intensity of the spectrum and $I(\omega_k)$ is the experimentally measured relative intensity of the spectrum. The summation was carried out over all ω_k points corresponding to the peaks of the comb spectrum where $I(\omega_k)$ exceeded threshold (e.g. −40 dB). Computations for modulation frequencies $\nu \sim$ 120 and 240 GHz yielded similar results. The best agreement between the calculated and measured spectra was obtained at $\beta_2(0) = -7.5$ ps^2 km^{-1} and $\beta_2(L) = 0$. In a similar way, we calculated the third-order dispersion parameter, constant along the length of the fibre, for the group velocity dispersion profile obtained: $\beta_3 = 0.015$ ps^3 km^{-1}. The calculated spectra corresponding to the propagation of modulated light in DDF with the optimised dispersion profile are shown in Fig. 5 along with the measured spectra.

4. Conclusions

Using a new sample of a silica DDF fabricated at PGPI, we have developed an experimental setup for high-frequency pulse train generation from initially modulated cw light in the telecom range. In our experiments, we have demonstrated the formation of stable contrast pulse trains with a repetition rate in the range 100–300 GHz and the generation of an optical comb spectrum with a −20-dB width of up to 80 nm. In addition, in our experiments the DDF sample has been successfully used to compress an individual pulse in a high-frequency train to a subpicosecond duration. The proposed configuration can be used as a basis for designing a family of comb spectrum generators and is of interest for telecommunications, spectroscopy, microwave photonics, and other applications.

The dispersion profile $\beta_2(z)$ of the DDF sample under consideration, as reconstructed from numerical simulation results, is in perfect agreement with the dispersion parameters intended in fibre drawing: low group velocity dispersion (GVD) throughout the length of the sample and near zero GVD at its narrow end. Moreover, the low third-order dispersion β_3 is quite consistent with the structure of the sample. The proposed approach for reconstructing the dispersion profile of fibre can be used as a high-speed method for the metrology of dispersion parameters of longitudinally nonuniform fibres.

Acknowledgements. We are grateful to our colleagues at the Prokhorov General Physics Institute, Russian Academy of Sciences, for supplying the DDF sample.

This work was supported by the RF Ministry of Science and Higher Education (Megagrant Programme, Application No. 2020-220-08-1369), the Russian Science Foundation (Grant No. 19-72-10037), and the Russian Foundation for Basic Research (Grant No. 19-42-730009).

References

1. Scott A.C. *The Nonlinear Universe: Chaos, Emergence, Life* (Berlin: Springer, 2007).
2. Tai K., Hasegawa A., Tomita A. *Phys. Rev. Lett.*, **56**, 135 (1986).
3. Agrawal G.P. *Nonlinear Fiber Optics* (San Diego: Academic, 1995; Moscow: Mir, 1996).
4. Marhic M.E. *Fiber Optical Parametric Amplifiers, Oscillators and Related Devices* (New York: Cambridge University Press, 2008).
5. Lugiato L.A., Lefever R. *Phys. Rev. Lett.*, **58**, 2209 (1987).
6. Bonatto C., Feyereisen M., Barland S., Giudici M., Masoller C., Rios Leite J.R., Tredicce J.R. *Phys. Rev. Lett.*, **107**, 053901 (2011).
7. Korobko D.A., Fotiadi A.A., Zolotovskii I.O. *Opt. Express*, **25**, 21180 (2017).
8. Kip D., Soljacic M., Segev M., Eugenieva E., Christodoulides D.N. *Science*, **290**, 495 (2000).
9. Clerc M.G., González-Cortés G., Wilson M. *Opt. Lett.*, **41**, 2711 (2016).
10. Malendevich R., Jankovic L., Stegeman G., Aitchison J.S. *Opt. Lett.*, **26**, 1879 (2001).
11. Zolotovskii I.O., Korobko D.A., Lapin V.A. *Quantum Electron.*, **44**, 42 (2014) [*Kvantovaya Elektron.*, **44**, 42 (2014)].
12. Tajima K. *J. Lightwave Technol.*, **4**, 900 (1986).

13. Mamyshev P.V., Chernikov S.V., Dianov E.M., Prokhorov A.M. *Opt. Lett*., **15**, 1365 (1990).
14. Närhi M., Wetzel B., Billet C., Toenger S., Sylvestre T., Merolla J.M., Dudley J.M. *Nat. Commun*., **7**, 1 (2016).
15. Mussot A., Conforti M., Trillo S., Copie F., Kudlinski A. *Adv. Opt. Photonics*, **10**, 1 (2018).
16. Swanson E.A., Chinn S.R. *IEEE Photonics Technol. Lett*., **6**, 796 (1994).
17. Lecaplain C., Grelu P. *Opt. Express*, **21**, 10897 (2013).
18. Korobko D.A., Stoliarov D.A., Itrin P.A., Odnoblyudov M.A., Petrov A.B., Gumenyuk R.V. *Opt. Laser Technol*., **133**, 106526 (2021).
19. Saarinen E.J., Rantamäki A., Chamorovskiy A., Okhotnikov O.G. *Electron. Lett*., **48**, 1355 (2012).
20. Peccianti M., Pasquazi A., Park Y., Moss D.J., Little B.E., Chu S.T., Morandotti R. *Nat. Commun*., **3**, 765 (2012).
21. Pasquazi A., Peccianti M., Razzari L., Moss D.J., Coen S., Erkintalo M., Morandotti R. *Phys. Rep*., **729**, 1 (2018).
22. Chernikov S.V., Dianov E.M., Richardson D.J., Laming R.I., Payne D.N. *Appl. Phys. Lett.*, **63**, 293 (1993).
23. Xu W., Zhang S., Chen W., Luo A., Liu S. *Opt. Commun*., **199**, 355 (2001).
24. Dudley J.M., Taylor J.R. *Supercontinuum Generation in Optical Fibers* (New York: Cambridge University Press, 2010).
25. Chernikov S.V., Mamyshev P.V. *J. Opt. Soc. Am. B*, **8**, 1633 (1991).
26. Chernikov S., Richardson D., Payne D., Dianov E. *Opt. Lett*., **18**, 476 (1993).
27. Korobko D.A., Okhotnikov O.G., Stoliarov D.A., Sysolyatin A.A., Zolotovskii I.O. *J. Opt. Soc. Am. B*, **32**, 692 (2015).
28. Zolotovskii I.O., Korobko D.A., Okhotnikov O.G., Sysolyatin A.A., Fotiadi A.A. *Quantum Electron*., **42**, 828 (2012) [*Kvantovaya Elektron*., **42**, 828 (2012)].
29. Yang C., Li W., Yu W., Liu M., Zhang Yu., Ma G., Lei M., Liu W. *Nonlinear Dyn.*, **92**, 203 (2018).
30. Akhmetshin U.G., Bogatyrev V.A., Senatorov A.K., Sysolyatin A.A., Shalygin M.G. *Quantum Electron*., **33**, 265 (2003) [*Kvantovaya Elektron*., **33**, 265 (2003)].
31. Fatome J., Pitois S., Fortier C., Kibler B., Finot C., Millot G., Courde C., Lintz M., Samain E. *Opt. Commun*., **283**, 2425 (2010).
32. Fatome J., Garnier J., Pitois S., Petit M., Millot G., Gay M., Clouet B., Bramerie L., Simon J.C. *Opt. Fiber Technol.*, **14**, 84 (2008).